Atmos. Chem. Phys. Discuss., https://doi.org/10.5194/acp-2018-696
Manuscript under review for journal Atmos. Chem. Phys.
Discussion started: 12 October 2018

Atmospheric Chemistry and Physics Discussions

Atmospheric Band Fitting Coefficients Derived from Self-Consistent Rocket-Borne Experiment

Mykhaylo Grygalashvyly[1], Martin Eberhart[5], Jonas Hedin[4], Boris Strelnikov[1], Franz-Josef Lübken[1], Markus Rapp[1,2], Stefan Löhle[5], Stefanos Fasoulas[5], Mikhail Khaplanov[4†], Jörg Gumbel[4], and Ekaterina Vorobeva[3]

[1]Leibniz-Institute of Atmospheric Physics at the University Rostock in Kühlungsborn, Schloss-Str. 6, D-18225 Ostseebad Kühlungsborn, Germany

[2]Deutsches Zentrum für Luft- und Raumfahrt, Institut für Physik der Atmosphäre, Oberpfaffenhofen, Germany

[3]Department of Atmospheric Physics, Saint-Petersburg State University, Universitetskaya Emb. 7/9, 199034, Saint-Petersburg, Russia

[4]Department of Meteorology (MISU), Stockholm University, Stockholm, Sweden

[5]University of Stuttgart, Institute of Space Systems, Stuttgart, Germany

[†]Deceased

Abstract

Based on self-consistent rocket-borne measurements of temperature, densities of atomic oxygen and neutral air, and volume emission of the Atmospheric Band (762 nm) we examined the one-step and two-step excitation mechanism of $O_2(b^1\Sigma_g^+)$ for night-time conditions. Following McDade et al. (1986), we derived the empirical fitting coefficients, which parameterize the Atmospheric Band emission $O_2(b^1\Sigma_g^+ - X^3\Sigma_g^-)(0,0)$ in terms of the atomic oxygen concentrations. This allows to derive atomic oxygen concentration from night-time observations of Atmospheric Band emission $O_2(b^1\Sigma_g^+ - X^3\Sigma_g^-)(0,0)$. The derived empirical parameters can also be utilised for Atmospheric Band modelling. Additionally, we derived fit function and corresponding coefficients for combined (one- and two-step)

Atmos. Chem. Phys. Discuss., https://doi.org/10.5194/acp-2018-696
Manuscript under review for journal Atmos. Chem. Phys.
Discussion started: 12 October 2018

Atmospheric Chemistry and Physics Discussions

mechanism. Simultaneous and true common volume measurements of all the parameters used in this derivation, i.e. temperature and density of the background air, atomic oxygen density, and volume emission rate, is the novelty and the advantage of this work.

1. Introduction

The mesopause region is essential to understand the chemical and physical processes in the upper atmosphere, as well as coupling between atmospheric layers. This region is characterised by different airglow emissions and, particularly, by emissions in the Atmospheric Band that form the excited state of molecular oxygen $O_2\left(b^1\Sigma_g^+\right)$. Airglow observation in the Atmospheric Band is a useful method to study dynamical processes in the mesopause region. There have been a number of reports of gravity waves (GWs) detection in this band (Noxon, 1978; Viereck and Deehr, 1989; Zhang et al., 1993). Planetary wave climatology has been investigated by the Spectral Airglow Temperature Imager (SATI) instrument (Lopez-Gonzales et al., 2009). In addition, the tides parameters have been reported from SATI (Lopez-Gonzales et al., 2005) and High Resolution Doppler Imager (HRDI) observations (Marsh et al., 1999). In numerous works Takahashi inferred the temperature by Atmospheric Band observation (Takahashi et al., 1990; 1992; 2011). Furthermore, the response of mesopause temperature and atomic oxygen during major sudden stratospheric warming was studied utilising Atmospheric Band emission by Shepherd et al. (2010). Various works have focused on Atmospheric Band emission modelling with respect to gravity waves and tides (e.g. Hickey et al., 1993; Leko et al., 2002; Liu and Swenson, 2003). The specific theory of the gravity wave effects on $O_2\left(b^1\Sigma_g^+\right)$ emission was derived in Tarasick and Shepherd (1992). Moreover, Atmospheric Band observations have been widely utilised to infer atomic oxygen, which is an essential chemical constituent for energetic balance in the extended mesopause region (e.g. Hedin et al., 2009, and references there in), and ozone

Atmos. Chem. Phys. Discuss., https://doi.org/10.5194/acp-2018-696
Manuscript under review for journal Atmos. Chem. Phys.
Discussion started: 12 October 2018

concentration (Mlynczak et al., 2001). Although there is a large field of application of Atmospheric Band emissions, there is a lack of knowledge on processes of the $O_2(b^1\Sigma_g^+)$ population. Two main mechanisms of population were proposed: the first is the direct population from three-body recombination of atomic oxygen (e. g. Deans et al., 1976); the second is the so-called two-step mechanism, which assumes an intermediate excited precursor O_2^* (e. g. Witt et al., 1984; Greer et al., 1981). It has been shown by laboratory experiments that the first mechanism alone has not explained observed emissions (Young and Sharpless, 1963; Clyne at al., 1965; Young and Black, 1966; Bates, 1988). The second mechanism entails a discussion about the precursor excited state and additional ambiguities in their parameters (e.g. Greer et al., 1981; Ogryzlo et al., 1984). Thus, Witt et al. (1984) proposed hypothesis that the $O_2(c^1\Sigma_u^-)$ state is, possibly, precursor; López-González et al. (1992a) suppose that the precursor could be $O_2(^5\Pi_g)$; Wildt et al. (1991) found by laboratory measurements that it could be $O_2(A^3\Sigma_u^+)$. Hence, the problem of identification is still not solved. The breakthrough has been done after the ETON 2 (Energy Transfer in the Oxygen Nightglow) rocket experiment. ETON 2 mission yielded empirical fitting parameters that allow to quantify the $O_2(b^1\Sigma_g^+)$ (and, consequently, volume emission) by known O or atomic oxygen by known volume emission (McDade et al., 1986). Despite the significance of this work, there was an ambiguity in the derived fitting parameters because the temperature and density of air (necessary for derivation) were taken from CIRA-72 and MSIS-83 models, which leads to the loss of self-consistency (e.g. Murtagh et al., 1990) and, consequently, to essential biases. Thus, more solid knowledge on these fitting coefficients based on consistent measurements of atomic oxygen, volume emission of Atmospheric Band, and temperature and density of background atmosphere is desirable. In this paper we present real common volume in-situ measurements of these parameters performed in the course of WADIS-2 sounding rocket mission. In the next chapter, we describe the rocket experiment and obtained

data relevant for our study. In chapter 3, to make the paper easier to understand, we repeat some theoretical approximations from McDade et al. (1986). The obtained results of our calculations are discussed in chapter 4. Concluding remarks and summary are given in the last chapter.

2. Rocket experiment Description

The WADIS (Wave propagation and dissipation in the middle atmosphere: Energy budget and distribution of trace constituents) sounding rocket mission aimed to simultaneously study the propagation and dissipation of GWs and measure the concentration of atomic oxygen. It comprised two field campaigns conducted at the Andøya Space Center (ASC) in northern Norway (69°N, 16°E). The WADIS-2 sounding rocket was launched during the second campaign on 5 March 2015 at 01:44:00 UTC, that is, night-time conditions. For a more detailed mission description, the reader is referred to Strelnikov et al. (2017) and the accompanying paper by Strelnikov et al. (2018).

The WADIS-2 sounding rocket was equipped with the CONE instrument to measure absolute neutral air density and temperature with high spatial resolution, instrument for atomic oxygen density measurements FIPEX (Flux Probe Experiment) and the Airglow Photometer for atmospheric band (762 nm) volume emission observation.

CONE (COmbined measurement of Neutrals and Electrons), operated by IAP (Leibniz Institute of Atmospheric Physics at the Rostock University), is a classical triode type ionisation gauge optimised for a pressure range between 10^{-5} to 1 mbar. The triode system is surrounded by two electrodes: Whilst the outermost grid is biased to +3 to +6 V to measure electron densities at a high spatial resolution, the next inner grid (-15 V) is meant to shield the ionisation gauge from ionospheric plasma. CONE is suitable for measureing absolute neutral air number densities at altitude range between 70 and 120 km. To obtain absolute densities,

the gauges are calibrated in the laboratory using a high-quality pressure sensor, like a Baratron. The measured density profile can be further converted to a temperature profile assuming hydrostatic equilibrium. For a detailed description of the CONE instrument, see Giebeler et al. (1993) and Strelnikov et al. (2013).

The Airglow Photometer operated by MISU (Stockholm University, Department of Meteorology) measures the emission of the molecular oxygen Atmospheric Band around 762 nm from the overhead column, from which volume emission rate is inferred by differentiation. A suitable description and review of this measurement technique is given by Hedin et al. (2009).

The aim of the FIPEX developed by the IRS (Institute of Space Systems, University of Stuttgart) is to measure the atomic oxygen density along the rocket trajectory with high spatial resolution. It employs two types of solid electrolyte sensors that differ in their electrode material. Platinum electrodes are sensitive to both molecular and atomic oxygen, whilst gold electrodes show a selective sensitivity to atomic oxygen. A low voltage is applied between anode and cathode pumping oxygen ions through the electrolyte ceramic (yttria stabilised zirconia). The current measured is proportional to the oxygen density. Sampling is realised with a frequency of 100 Hz and enables a spatial resolution of ~10 m. Laboratory calibrations were done for molecular and atomic oxygen. For a detailed description of the FIPEX instruments and their calibration techniques see Eberhart et al. (2015, 2018).

3. Theory

Here, we are repeating the theory of $O_2\left(b^1\Sigma_g^+ - X^3\Sigma_g^-\right)(0,0)$ night-time emissions following McDade et al. (1986) to make our paper more readable, saving all nomenclature as in the original paper. All utilised reactions are listed in Table 1, together with corresponding reaction rates, branching ratios, quenching rates and spontaneous emission coefficients. Some

Atmos. Chem. Phys. Discuss., https://doi.org/10.5194/acp-2018-696
Manuscript under review for journal Atmos. Chem. Phys.
Discussion started: 12 October 2018

Atmospheric Chemistry and Physics Discussions

components have been updated according to modern knowledge, thus, deviating from the work of McDade et al. (1986).

Assuming direct one-step mechanism as a main one for population of $O_2\left(b^1\Sigma_g^+\right)$, we can write its concentration as a ratio of production to the loss term:

$$\left[O_2\left(b^1\Sigma_g^+\right)\right] = \frac{\varepsilon k_1 [O]^2 M}{A_2 + k_2^{O_2}[O_2] + k_2^{N_2}[N_2] + k_2^{O}[O]}, \quad (1)$$

where k_1 – reaction rate for three-body recombination of atomic oxygen, ε is the corresponding fraction of recombination, A_2 represents the spontaneous emission coefficient, and $k_2^{O_2}, k_2^{N_2}, k_2^{O}$ are the quenching coefficients for reactions with O_2, N_2 and O, respectively.

The volume emission for transition $O_2\left(b^1\Sigma_g^+ - X^3\Sigma_g^-\right)(0,0)$ is a product of the concentration of excited molecules and the spontaneous emission coefficient for the given transition:

$$V_{at} = A_1\left[O_2\left(b^1\Sigma_g^+\right)\right] = \frac{A_1 \varepsilon k_1 [O]^2 M}{A_2 + k_2^{O_2}[O_2] + k_2^{N_2}[N_2] + k_2^{O}[O]}, \quad (2)$$

where A_1 is spontaneous emission for reaction R5 (hereafter, nomenclature RX means the reaction X from Table 1). In case of known temperature, volume emission and concentrations of O, O_2, N_2, and M, the fraction of recombination can be calculated as follows:

$$\varepsilon = V_{at} \frac{A_2 + k_2^{O_2}[O_2] + k_2^{N_2}[N_2] + k_2^{O}[O]}{A_1 k_1 [O]^2 M}. \quad (3)$$

In the case of the two-step mechanism, the unknown excited state O_2^* is populated at the first step from the reaction R7. Then, it can be deactivated by quenching (R9), spontaneous emission (R10) or producing $O_2\left(b^1\Sigma_g^+\right)$ by the reaction R8. The concentration of these excited molecules is given by the following expression:

$$[O_2^*] = \frac{\alpha k_1 [O]^2 M}{A_3 + k_3^{O_2}[O_2] + k_3^{N_2}[N_2] + k_3^{O}[O]}, \quad (4)$$

where fraction of recombination α, spontaneous emission coefficient A_3, quenching rates $k_3^{O_2}, k_3^{N_2}, k_3^{O}$ – are unknown values, as well as the precursor excited state.

Atmos. Chem. Phys. Discuss., https://doi.org/10.5194/acp-2018-696
Manuscript under review for journal Atmos. Chem. Phys.
Discussion started: 12 October 2018

Atmospheric Chemistry and Physics Discussions

In the second step, O_2^* is transformed into $O_2\left(b^1\Sigma_g^+\right)$, which, in turn, can be deactivated by quenching (R2-R4) and by spontaneous emission (R6). Its concentration in the case of the two-step mechanism is:

$$\left[O_2\left(b^1\Sigma_g^+\right)\right] = \frac{\gamma k_3^{O_2}[O_2][O_2^*]}{A_2 + k_2^{O_2}[O_2] + k_2^{N_2}[N_2] + k_2^{O}[O]}. \quad (5)$$

The volume emission in the case of $O_2\left(b^1\Sigma_g^+ - X^3\Sigma_g^-\right)(0,0)$ is:

$$V_{at} = \frac{A_1 \alpha k_1[O]^2 M \gamma k_3^{O_2}[O_2]}{\left(A_2 + k_2^{O_2}[O_2] + k_2^{N_2}[N_2] + k_2^{O}[O]\right)\left(A_3 + k_3^{O_2}[O_2] + k_3^{N_2}[N_2] + k_3^{O}[O]\right)}. \quad (6)$$

Collecting all known values on the right-hand side (RHS) and all unknown summands on the left-hand side (LHS), equation (6) can be rearranged as follows:

$$\frac{A_3 + k_3^{O_2}[O_2] + k_3^{N_2}[N_2] + k_3^{O}[O]}{\alpha\gamma k_3^{O_2}} = \frac{A_1 k_1[O]^2 M[O_2]}{V_{at}\left(A_2 + k_2^{O_2}[O_2] + k_2^{N_2}[N_2] + k_2^{O}[O]\right)}. \quad (7)$$

Omitting emissive summand A_3 as non-effective loss (McDade et al., 1986) we can transform (7) into the following expression:

$$C^{O_2}[O_2] + C^{O}[O] = \frac{A_1 k_1[O]^2 M[O_2]}{V_{at}\left(A_2 + k_2^{O_2}[O_2] + k_2^{N_2}[N_2] + k_2^{O}[O]\right)}, \quad (8)$$

where $C^{O_2} = \left(1 + k_3^{N_2}[N_2]/k_3^{O_2}[O_2]\right)/\alpha\gamma$ and $C^{O} = k_3^{O}/\alpha\gamma k_3^{O_2}$ are the fitting coefficients that can be calculated by the least square fit (LSF) procedure. We calculated them based on our measurements and will discuss the results in the following chapter.

4. Results and Discussion

Figure 1 shows input data for our calculations: temperature from CONE instrument (Fig. 1a), number density of air (Fig. 1b), atomic oxygen concentration measured by FIPEX (Fig. 1c) and volume emission at 762 nm from photometric instrument (Fig. 1d). A temperature minimum of ~158 K was observed at 104.2 km. A local temperature peak was measured at

98.9 km with values of 204.5 K. The secondary temperature minimum was visible at 95.4 km and amounted to ~173 K. Atomic oxygen concentration (Fig. 1c) had a peak of ~$4.7 \cdot 10^{11}$ [cm^{-3}] at 97.2 km and approximately coincided with the secondary temperature peak. The peak of volume emission was detected between 95 and 97 km with values of more than 1700 [$phot. \cdot cm^{-3} \cdot s^{-1}$]; this is slightly beneath the atomic oxygen corresponding maximum and slightly above the secondary temperature minimum. Note, this point to the competition of the temperature and the atomic oxygen concentration in the processes of atomic oxygen excited state $O_2\left(b^1\Sigma_g^+\right)$ formation. Independently of the mechanism of atmospheric band emission (Eq. 2 or Eq. 6), the numerator is directly proportional to the square of atomic oxygen concentration and inversely proportional to the third power of the temperature (via reaction rate k_1 and M, considering the ideal gas low). Our rocket experiment shows an essential difference of emissions between ascending and descending flights (see Strelnikov et al., 2018). It also demonstrates a significant variability in other measured parameters, including neutral temperature and density as well as atomic oxygen density. This suggests that, in the case of the ETON 2 experiments, the temporal extrapolation of atomic oxygen for the time of the emission measurement flight (which was approximately 20 min earlier) may lead to serious biases in estimations because, as one can see from Eq. 2 and Eq. 6, volume emission depends on the atomic oxygen concentration quadratically. Since the best quality data were obtained during the descent of the WADIS-2 rocket flight, we chose this data set for our analysis (Strelnikov et al., 2018). The region above 104 km is subject to auroral contamination. In the region below 92 km, negative values may occur in the volume emission profile as the result of self-absorption in the denser atmosphere below the emission layer. Hence, we considered the region near the peak of emission between 92 km and 104 km as most appropriate for our study. The comparisons of our measurements with other observations, as well as with the results of modelling are presented in several papers (e.g. Eberhart et al., 2018; Strelnikov et al., 2018).

Atmos. Chem. Phys. Discuss., https://doi.org/10.5194/acp-2018-696
Manuscript under review for journal Atmos. Chem. Phys.
Discussion started: 12 October 2018

Atmospheric Chemistry and Physics Discussions

191

192 **4.1 One-step mechanism**

193

194 Figure 2 shows the fraction of recombination ε calculated according to Eq. (3), which is
195 necessary to form $O_2\left(b^1\Sigma_g^+\right)$ under the assumption that the direct three-body recombination of
196 atomic oxygen is the main mechanism. As is expected, ε is scattered approximately in the
197 range [0.07; 0.13], which is in good agreement with the values derived by McDade et al.
198 (1986). The averaged value amounts to 0.1. By the physical nature of this value, the fraction
199 of recombination should not depend on altitude, but Fig. 2 shows the strong altitude
200 dependence. Such behaviour of ε means that measured atmospheric emissions may not be
201 explained merely in light of direct excitation mechanism if ε is independent of temperature.
202 Hence, we plot values of ε depending on measured temperature in Figure 3. The values are
203 distributed not randomly and show clear functional dependence. This dependence has a
204 complex nonlinear form. The spiral shape points to the existence of a second parameter,
205 which is probably the pressure. The reaction rates in general cases are the functions of
206 temperature and pressure (e. g. Troe, 1979). Hence, ε, which represents the ratio of the
207 reaction rates of different branches, must depend, in general, on temperature and pressure.
208 Correct functional relation $\varepsilon = \varepsilon(T, p)$ can be obtained only through laboratory
209 measurements. In light of the analysis of our rocket experiment, we can only state that such
210 functional dependence may exist. Hence, an explanation of atmospheric band emission via
211 one-step mechanism is, generally speaking, possible. On the other hand, an existence of
212 functional dependence is the necessary but not sufficient condition to state that the one-step
213 mechanism populates $O_2\left(b^1\Sigma_g^+\right)$. Moreover, although the population via one-step mechanism
214 alone is possible, it is improbable because laboratory experiments show that the direct
215 excitation alone may not explain observed emissions (Young and Sharpless, 1963; Clyne at

al., 1965; Young and Black, 1966; Bates, 1988). This conclusion is partially in agreement with the conclusion from McDade et al. (1986), which stated that the one-step excitation mechanism is not sufficient to explain the $O_2\left(b^1\Sigma_g^+\right)$ population.

The reason of some inconsistency between our and McDade et al. (1986) formulation is that, in the case of ETON 2 experiments it was not possible to correlate ε with the real temperature at the place and in time of rocket launch. For their analysis, mean temperature profiles were utilised from the models CIRA-72 and MSIS-83 (Hedin, 1983), which does not reproduce any short-time dynamical fluctuations, solar cycle conditions, etc. Hence, the investigation of correlation between temperature and ε was not possible. Therefore, just in frame of our experiment, we may not decline that $O_2\left(b^1\Sigma_g^+\right)$ is populated via one-step or other mechanisms, but taking into account the results of laboratory measurements Bates (1988) and theoretical investigations Wraight (1982), which infer too low ε (0.03 and 0.015, respectively) we should conclude that one-step mechanism alone does not explain observed emissions. Hence, in the following, we check the second energy transfer mechanism.

4.2 Two-step mechanism

Figure 4 depicts the altitude profile of the RHS of equation (8) and profile calculated by the least-square fit (LSF). The fitting coefficients, C^{O2} and C^{O}, resulting from this fit, are amount to 9.8 and 2.1, respectively. In such a way defined (Eq. 8) fitting coefficients do not have a direct physical meaning. However, they have a physical meaning in several limit cases. If the quenching coefficients of a precursor with molecular nitrogen are much smaller than those with molecular oxygen $\left(k_3^{N_2} \ll k_3^{O_2}\right)$, then $\alpha\gamma = 1/C^{O2}$. In our case $\alpha\gamma = 0.102$. In other words, in the case of two-step formation of $O_2\left(b^1\Sigma_g^+\right)$ with energy transfer agent O_2, the total efficiency $\alpha\gamma$ amounts to 10.2%, which is the lowest amongst known values. Based on rocket

Atmos. Chem. Phys. Discuss., https://doi.org/10.5194/acp-2018-696
Manuscript under review for journal Atmos. Chem. Phys.
Discussion started: 12 October 2018

Atmospheric Chemistry and Physics Discussions

241 experiment data analysis (ETON), Witt et al. (1984) obtained $\alpha\gamma = 0.12 - 0.2$. According to
242 McDade et al. (1986), for the case with $k_2^O = 8 \cdot 10^{-14}$, the total efficiencies are 0.15 and
243 0.21 for temperature profiles adopted from MSIS-83 and CIRA-72, respectively. The analyses
244 of López-González et al. (1992a, c), adopted O_2, N_2, and temperature profiles from the model
245 (Rodrigo et al., 1991), showed a total efficiency of 0.16. In contrast to our work, all
246 investigations mentioned above utilised the temperature and atmospheric density from models
247 which describe a mean state of the atmosphere. This is a possible reason for discrepancy in
248 the results. Total efficiency may serve as an auxiliary quantity to identify the precursor.
249 According to the physical meaning of efficiency, it may not be larger than 1. Hence, α, γ, as
250 well as the total efficiency are smaller than 1. Consequently, $\gamma = tot.eff./\alpha < 1$, and we
251 can examine potential candidates for O_2^* with this criterion. From an energetic point of view,
252 only four bound states of molecular oxygen can be considered as an intermediate state for the
253 $O_2\left(b^1\Sigma_g^+\right)$ population: $O_2(A^3\Sigma_u^+), O_2(A'^3\Delta_u), O_2(c^1\Sigma_u^-)$, and $O_2(^5\Pi_g)$ (Greer et al., 1981;
254 Wraight, 1982; Witt et al., 1984; McDade et al., 1986; López-González et al., 1992c). For
255 better readability, we will partially repeat a table from López-González et al. (1992b, c) with
256 known α in our work (Table 2). From Table 2, it can be seen that only $O_2(A'^3\Delta_u)$ and
257 $O_2(^5\Pi_g)$ fit to the criterion of $\gamma = 0.102/\alpha < 1$.
258 The second expression that helps to clarify the choice of the precursor is the ratio of
259 quenching rates. In the limit of low quenching with molecular nitrogen $\left(k_3^{N_2} \ll k_3^{O_2}\right)$, the ratio
260 of fitting coefficients equals the ratio of the quenching rates of atomic and molecular oxygens
261 $\left(C^O/C^{O2} = k_3^O/k_3^{O_2}\right)$. An analysis from the ETON 2 rocket experiment yields values of
262 quenching coefficients ratios of potential precursor are 3.1 and 2.9 for temperatures from
263 CIRA-72 and MSIS-83, respectively. This is close to the value from Ogryzlo et al. (1984),
264 who found $k_3^O/k_3^{O_2} = 2.6$ by laboratory measurements; however, as was noted in their work,
265 substitution of these values into the equation for emission yields 16 % of the observed

Atmos. Chem. Phys. Discuss., https://doi.org/10.5194/acp-2018-696
Manuscript under review for journal Atmos. Chem. Phys.
Discussion started: 12 October 2018

Atmospheric Chemistry and Physics Discussions

emission (Ogryzlo et al., 1984). These findings point to the possibility of a too high measured ratio $k_3^O/k_3^{O_2}$ as the result of too strong quenching of precursor by atomic oxygen. Our value of quenching ratios $k_3^O/k_3^{O_2}$ amounts to 0.21. There is not enough information on measured values for bound states of molecular oxygen. Laboratory measurements for $O_2(A^3\Sigma_u^+)(v = 0-4)$, $O_2(A^3\Sigma_u^+)(v = 2)$, and $O_2(c^1\Sigma_u^-)$ infer the values of $k_3^O/k_3^{O_2}$ ratio to be 30±30, 100±15, and 200±20, respectively (Kenner and Ogryzlo, 1980; Kenner and Ogryzlo, 1983a, 1983b; Kenner and Ogryzlo, 1984). On the other hand, Slanger et al. (1984) found a lower limit of $O_2(A^3\Sigma_u^+)(v = 8)$ quenching by O_2 must be $\geq 8 \cdot 10^{-11}$. If the results from Slanger et al. (1984) were applied to the results from Kenner and Ogryzlo (1980, 1984) for $k_3^{O_2}$, then the ratio of $k_3^O/k_3^{O_2}$would be two orders lower. This short discussion illustrates a strong scattering of this ratio. For our two potential candidates ($O_2(A'^3\Delta_u)$ and $O_2(^5\Pi_g)$), there is information about $k_3^O/k_3^{O_2}$ ratio for only $O_2(A'^3\Delta_u)$. Through the comprehensive analysis of known rocket experiments, López-González et al. (1992a, b, c) inferred that the upper limit of the ratio amounts to 1. Hence, our value of $k_3^O/k_3^{O_2} = 0.21$ agrees with this result. Consistent information from laboratory experiments on the ratio for $O_2(^5\Pi_g)$ is absent. Thus, we can propose as potential candidates for precursor both $O_2(A'^3\Delta_u)$ and $O_2(^5\Pi_g)$; however, we are not able to identify which of these two is more preferable.

In order to illustrate the application of the newly derived fitting coefficients we show Figure 5 with atomic oxygen concentration from FIPEX (black line), from NRL MSISE-00 reference atmosphere model (Picone et al., 2002) (red line); calculated with McDade et al. (1986) coefficients (blue line), and with our fitting coefficients for the two-step mechanism (green line). In the region 90-98 km, i.e. beneath atomic oxygen peak (see Fig. 1d) fitting coefficients from this paper better then McDade coefficients (MSIS-83 case). Our fitting coefficients and fitting coefficients of McDade give similar approximation above atomic

oxygen peak (~98-104 km). The atomic oxygen retrieved with our fitting coefficients satisfactorily reproduces measurements.

4.3 Combined mechanism

In the most general case, the $O_2(b^1\Sigma_g^+)$ population passes through two channels: directly and via precursor. In fact, theoretical calculations from Wraight (1982) and laboratory measurements from Bates (1988) predicted a direct population with efficiencies of 0.015 and 0.03, respectively, which is not sufficient to explain the observed emissions (Bates, 1988, Greer et al., 1981; Krasnopolsky, 1986). A similar value, ε=0.02, was shown in the analysis by López-González et al. (1992b, c). We investigated a combined mechanism based on the LSF calculation and fit function (derivation in Appendix):

$$\frac{[O_2] + D_1[O]}{D_2 + \tilde{\varepsilon}(1 + D_1\,[O]/[O_2])} = \frac{A_1 k_1 [O]^2 M [O_2]}{V_{at}\left(A_2 + k_2^{O_2}[O_2] + k_2^{N_2}[N_2] + k_2^{O}[O]\right)}, \quad (9)$$

where, hereafter, tildes denote that these are values for combined mechanism and do not equal to the values for one-step or two-step mechanisms (Ch. 4.1 and 4.2); $D_1 = \tilde{k}_3^O/\tilde{k}_3^{O_2}$ and $D_2 = \tilde{\alpha}\tilde{\gamma}$ are the fitting coefficients, which refer to the ratio of quenching rates and total efficiency for two-step channel, respectively. The fitting coefficients were calculated for two limit cases $\tilde{\varepsilon}$=0.015 (Wraight, 1982), $\tilde{\varepsilon}$=0.03 (Bates, 1988) and for the averaged case $\tilde{\varepsilon}$=0.022. They are listed in Table 3. The altitude profile of the RHS of equation (9) and calculated fit-function are plotted in Figure 6. The deviations of fit function between limits and averaged values are negligible, hence, we only show the averaged case. Thus, we can recommend for future investigations the values of averaged case (last column of Tab. 3). Analogously to the two-step mechanism (Ch. 4.2), for the case of combined mechanism $\tilde{\gamma} = tot.eff./\tilde{\alpha} < 1$. Taking into account the lowest value for total efficiency, the precursor should satisfy $\tilde{\alpha} > 0.073$. Consequently, only $O_2(A'^3\Delta_u)$ and $O_2(^5\Pi_g)$ satisfy this criterion (see Tab 2). The upper limit of the ratio $k_3^O/k_3^{O_2} < 1$ for $O_2(A'^3\Delta_u)$, derived by López-González et al. (1992a,

b, c), is in agreement with our calculations (~0.2-0.4). As it is noted above, the ratio for $O_2(^5\Pi_g)$ is unknown.

Figure 7 illustrates volume emissions derived (black lines) with fitting coefficients of McDade et al. (1986) for MSIS-83 (Fig. 7c) case and CIRA-72 case (Fig. 7d), and with our newly derived fitting coefficients for two-step (Fig. 7a) and combined ($\tilde{\varepsilon} = 0.022$) mechanisms (Fig. 7b) in comparison with measured one (red lines). All of derived volume emission profiles (black lines) were calculated based on the the temperature, concentration of surrounding air, and concentration of atomic oxygen from our rocket launch. The calculations with combined mechanism (Eq. 9) and two-step energy transfer mechanism (Eq. 8) give almost identical results. The results obtained with new fitting coefficients are in satisfactory agreement with the measured volume emissions at the peak and above, whereas the McDade coefficients related to the temperature from CIRA-72 give better approximations below the volume emission peak (92 km). The coefficients of McDade related to the temperature from MSIS-83 are in better agreement with our results and are almost identical above the volume emission peak. Note that both mechanisms with newly derived coefficients give three of five points in the vicinity of uncertainties of measured values (see Fig. 7a and Fig 7b), whereas McDade coefficients for MSIS-83 case (Fig. 7c) and for CIRA-72 (Fig. 7d) give just one and two point, respectively. Hence, we can recommend our newly derived coefficients either for a two-step energy transfer process or for combined mechanism. We consider combined mechanism more preferable as it is more general.

5. Summary and conclusions

Based on the rocket-born true common volume observations of atomic oxygen, atmospheric band emission (762 nm), and density and temperature of the background atmosphere, the one-step, two-step and combined mechanisms of $O_2\left(b^1\Sigma_g^+\right)$ formation were analysed. Our

calculations show that in the case of the one-step mechanism, the fraction of atomic oxygen recombination ε depends on altitude. The one-step mechanism inferred the functional dependence of ε on temperature. It has a nonlinear character because the fraction of recombination ε, in general, depends on temperature and pressure. Nevertheless, we consider one-step direct excitation as less probable for the reasons discussed above (Ch.4.1). In the context of the rocket experiment, we do not have a possibility to retrieve functional dependence $\varepsilon = \varepsilon(T, p)$, which poses a task for future laboratory measurements.

For the case of the two-step mechanism, we found new coefficients for fit function in accordance with McDade et al. (1986), based on self-consistent temperature, atomic oxygen and volume emission observation. These coefficients amounted to C^{O2}=9.8 and C^{O}=2.1. The general implication of these results is parameterisation of volume emission in terms of known atomic oxygen. This can be utilised either for atmospheric band volume emission modelling or for estimation of atomic oxygen by known volume emission. We identified two candidates for the intermediate state of O_2^*. Our results show that $O_2(A'^3\Delta_u)$ or $O_2(^5\Pi_g)$ may serve as a precursor.

Taking into account both channels of $O_2\left(b^1\Sigma_g^+\right)$ formation, we proposed a combined mechanism. In this case, atomic oxygen via volume emission or volume emission based on known atomic oxygen can be calculated by equation (9). Recommended fitting coefficients amounted to D_1=0.231 and D_2=0.08, with the efficiency of the direct channel as $\tilde{\varepsilon} = 0.022$. These coefficients have a sense of total efficiency ($\tilde{\alpha}\tilde{\gamma}$) and a ratio of quenching coefficients ($\tilde{k}_3^O/\tilde{k}_3^{O_2}$) for the two-step channel. The analysis of their values indicates that $O_2(A'^3\Delta_u)$ and $O_2(^5\Pi_g)$ may serve as possible precursors for the two-step channel. Unfortunately, in the context of our rocket experiment, we do not have the possibility to figure out which mechanism is true. Nevertheless, we consider the combined mechanism as more relevant to nature, because it has a higher generality. This conclusion does not

Atmos. Chem. Phys. Discuss., https://doi.org/10.5194/acp-2018-696
Manuscript under review for journal Atmos. Chem. Phys.
Discussion started: 12 October 2018

365 contradict to the current point of view that the two-step mechanism is dominant because $\tilde{\varepsilon}$ is
366 assumed to be 1.5-3 %. Moreover, it is possible that in the reality the mechanism much more
367 complex and it has multi-channel or more than two-step nature.

368

369 **Appendix.**

370

371 We consider photochemical equilibrium for the night-time $O_2(b^1\Sigma_g^+)$ concentration. If
372 $O_2(b^1\Sigma_g^+)$ is produced via both channels, the equilibrium concentration is given by the
373 following expression:

$$[O_2(b^1\Sigma_g^+)] = \frac{\tilde{\varepsilon}k_1[O]^2M + \tilde{\gamma}\tilde{k}_3^{O_2}[O_2][O_2^*]}{A_2 + k_2^{O_2}[O_2] + k_2^{N_2}[N_2] + k_2^{O}[O]}, \qquad (A1)$$

374 where the tilde denotes the combined mechanism, $A_1, k_1, k_2^{O_2}, k_2^{N_2}, k_2^{O}, \tilde{k}_3^{O_2}$ are the ratios for
375 corresponding processes (see Tab. 1) and O_2^* is the unknown precursor.
376 Considering this precursor in photochemical equilibrium, we can obtain the following
377 expression for its concentration:

$$[O_2^*] = \frac{\tilde{\alpha}k_1[O]^2M}{\tilde{A}_3 + \tilde{k}_3^{O_2}[O_2] + \tilde{k}_3^{N_2}[N_2] + \tilde{k}_3^{O}[O]}, \qquad (A2)$$

378 where efficiency $\tilde{\alpha}$, $\tilde{A}_3$ is the unknown spontaneous emission coefficient of O_2^* and
379 $\tilde{k}_3^{O_2}, \tilde{k}_3^{N_2}, \tilde{k}_3^{O}$ are the unknown quenching rates for O_2^*.
380 Substituting A2 into A1 and into expression for volume emission we obtain:
381 $V_{at} = A_1[O_2(b^1\Sigma_g^+)] =$

$$= \frac{A_1k_1[O]^2[O_2]M}{A_2 + k_2^{O_2}[O_2] + k_2^{N_2}[N_2] + k_2^{O}[O]}\left(\frac{\tilde{\varepsilon}}{[O_2]} + \frac{\tilde{\alpha}\tilde{\gamma}\tilde{k}_3^{O_2}}{\tilde{A}_3 + \tilde{k}_3^{O_2}[O_2] + \tilde{k}_3^{N_2}[N_2] + \tilde{k}_3^{O}[O]}\right). \qquad (A3)$$

382 We assume that, in analogy with two-step mechanism, a spontaneous emission $\widetilde{A_3}$ of O_2^* is
383 much smaller than the quenching, and we utilised traditional assumption about low quenching

with molecular nitrogen $\left(\tilde{k}_3^{N_2} \ll \tilde{k}_3^{O_2}\right)$, which is commonly used to analyse a potential precursor. In this case, A3 can be rearranged as follows:

$$\frac{[O_2] + \frac{\tilde{k}_3^O}{\tilde{k}_3^{O_2}}[O]}{\tilde{\alpha}\tilde{\gamma} + \tilde{\varepsilon}\left(1 + \frac{\tilde{k}_3^O}{\tilde{k}_3^{O_2}}[O]/[O_2]\right)} = \frac{A_1 k_1 [O]^2 M [O_2]}{V_{at}\left(A_2 + k_2^{O_2}[O_2] + k_2^{N_2}[N_2] + k_2^O[O]\right)}. \quad (A4)$$

We defined unknown fitting coefficients $D_1 \equiv \tilde{k}_3^O / \tilde{k}_3^{O_2}$ and $D_2 \equiv \tilde{\alpha}\tilde{\gamma}$. Expression A4 was utilised to calculate them with LSF.

Acknowledgements.

The authors are thankful to Prof. Dr. V. A. Yankovsky, Prof. Dr. W. Ward, and PD Dr. G. R. Sonnemann for helpful suggestions and useful discussions. This work was supported by the German Space Agency (DLR) under grant 50 OE 1001 (project WADIS). The authors thank DLR-MORABA for their excellent contribution to the project by developing the complicated WADIS payload and campaign support together with the Andøya Space Center, as well as H.-J. Heckl and T. Köpnick for building the rocket instrumentation.

The rocket-borne measurements and calculated data shown in this paper are available via IAP's ftp server at ftp://ftp.iap-kborn.de/data-in-publications/GrygalashvylyACP2018.

References

Bates, D. R.: Excitation and quenching of the oxygen bands in the nightglow, *Planet. Space Sci.*, **36(9)**, 875-881, 1988.

Campbell, I. M. and Gray, C. N.: Rate constants for O(^{3}P) recombination and association with N(4S), Chem. Phys. Lett., **8**, 259, 1973.

Clyne, M. A. A., Thrush, B. A., and Wayne, R. P.: The formation and reactions of metastable oxygen $\left(b^1\Sigma_g^+\right)$ molecules, *J. Photochem. Photobiol.*, **4**, 957, 1965.

Deans, A. J., Shepherd, G. G., and Evans, W. F. J.: A rocket measurement of the $O_2\left(b^1\Sigma_g^+ - X^3\Sigma_g^-\right)$ atmospheric band nightglow altitude distribution, *Geophys. Res. Lett.*, **3(8)**, 441-444, 1976.

Eberhart, M., Löhle, S., Steinbeck, A., Binder, T., and Fasoulas, S.: Measurement of atomic oxygen in the middle atmosphere using solid electrolyte sensors and catalytic probes, *Atmospheric Measurement Techniques*, **8**, 3701–3714, doi:10.5194/amt-8-3701-2015, 2015.

Eberhart, M., Löhle, S., Strelnikov, B., Fasoulas, S. and Lübken, F.-J. Hedin, J., Khaplanov, M., Gumbel, J.: Atomic oxygen number densities in the MLT region measured by solid electrolyte sensors on WADIS-2, *Atmospheric Measurement Techniques*, submitted, 2018.

Giebeler, J., Lübken, F.-J., and Nägele, M.: CONE – a new sensor for in-situ observations of neutral and plasma density fluctuations, ESA SP, Montreux, Switzerland, ESA-SP-355, 311–318, 1993.

Greer, R. G. H., Llewellyn, E. J., Solheim, B. H., and Witt, G.: The excitation of $O_2\left(b^1\Sigma_g^+\right)$ in the nightglow, *Planet. Space Sci.*, **29**, 383, 1981.

Hedin, A. E.: A revised thermospheric model based on mass spectrometer and incoherent scatter data: MSIS-83, *J. Geophys. Res.*, **88**, 10.170, 1983.

Hedin, J., Gumbel, J., Stegman, J., and Witt, G.: Use of O_2 airglow for calibrating direct atomic oxygen measurements from sounding rockets, *Atmos. Meas. Tech.*, **2**, 801–812, 2009.

Hickey, M. P., Schubert, G., and Walterscheid, R. L.: Gravity wave-driven fluctuations in the O_2 atmospheric (0–1) nightglow from an extended, dissipative emission region, *J. Geophys. Res.*, **98**, 717–730, 1993.

Kenner, R. D. and Ogryzlo, E. A.: Deactivation of $O_2(A^3\Sigma_u^+)$ by O_2, O and Ar, *Int. J. Chem. Kinetics*, **12**, 501, 1980.

Kenner, R. D. and Ogryzlo, E. A.: Quenching of $O_2(c^1\Sigma_u^-, v = 0)$ by O(^{3}P), $O_2(a^1\Delta_g)$ and other gases, *Can. J. Chem.*, **61**, 921, 1983a.

Kenner, R. D. and Ogryzlo, E. A.: Rate constant for the deactivation of $O_2(A^3\Sigma_u^+)$ by N_2, *Chem. Phys. Lett.*, **103**, 209, 1983b.

Kenner, R. D. and Ogryzlo, E. A.: Quenching of $O_2(A_{v=2} - X_{v=5})$ Herzberg I band by O_2(a) and O, *Can. J. Phys.*, **62**, 1599, 1984.

Krasnopolsky, V. A.: Oxygen emissions in the night airglow of the Earth, Venus and Mars, *Planet. Space Sci.*, **34**, 511, 1986.

Leko, J. J., M. P. Hickey, and Richards, P. G.: Comparison of simulated gravity wave-driven mesospheric airglow fluctuations observed from the ground and space, *J. Atmos. Solar-Terr. Phys.*, **64**, 397– 403, 2002.

458

459 Liu, A. Z. and Swenson, G. R.: A modeling study of O_2 and OH airglow perturbations
460 induced by atmospheric gravity waves, *J. Geophys, Res.*, **108(D4)**, 4151,
461 doi:10.1029/2002JD002474, 2003.

462

463 López-González, M. J., López-Moreno, J. J., and Rodrigo, R.: Altitude profiles of the
464 atmospheric system of O_2 and of the green line emission, *Planet. Space Sci.*, **40(6)**, 783-795,
465 1992a.

466

467 López-González, M. J., López-Moreno, J. J., and Rodrigo, R.: Altitude and vibrational
468 distribution of the O_2 ultraviolet nightglow emissions, *Planet. Space Sci.*, **40(7)**, 913-928,
469 1992b.

470

471 López-González, M. J., López-Moreno, J. J., and Rodrigo, R.: Atomic oxygen concentrations
472 from airglow measurements of atomic and molecular oxygen emissions in the nightglow,
473 *Planet. Space Sci.*, **40(7)**, 929-940, 1992c.

474

475 Lopez-Gonzalez, M. J., Rodríguez, E., Shepherd, G. G., Sargoytchev, S., Shepherd, M. G.,
476 Aushev, V. M., Brown, S., García-Comas, M., and Wiens, R. H.: Tidal variations of O_2
477 Atmospheric and OH(6-2) airglow and temperature at mid-latitudes from SATI observations,
478 *Ann. Geophys.*, **23**, 3579–3590, 2005.

479

480 Lopez-Gonzalez, M. J., Rodríguez, E., García-Comas, M., Costa, V., Shepherd, M. G.,
481 Shepherd, G. G., Aushev, V. M., and Sargoytchev, S.: Climatology of planetary wave type
482 oscillations with periods of 2-20 days derived from O_2 atmospheric and OH(6-2) airglow
483 observations at mid-latitude with SATI, *Ann. Geophys.*, **27**, 3645–3662, 2009.

McDade, I. C., Murtagh, D. P., Greer, R. G. H., Dickinson, P. H. G., Witt, G., Stegman, J., Llewellyn, E. J., Thomas, L., and Jenkins, D. B.: ETON 2: Quenching parameters for the proposed precursors of $O_2(b^1\Sigma_g^+)$ and $O(^1S)$ in the terrestrial nightglow, *Planet. Space Sci.*, **34**, 789–800, 1986.

Mlynczak, M. G., Morgan, F., Yee, J.-H., Espy, P., Murtagh, D., Marshall, B., Schmidlin, F.: Simultaneous measurements of the $O_2(^1\Delta)$ and $O_2(^1\Sigma)$ airglows and ozone in the daytime mesosphere, *Geophys. Res. Lett.*, **28**, 999-1002, 2001.

Murtagh, D. P., Witt, G., Stegman, J., McDade, I. C., Llewellyn, E. J., Harris, F., and Greer, R. G. H.: An assessment of proposed $O(^1S)$ and $O_2(b^1\Sigma_g^+)$ nightglow excitation parameters, *Planet. Space Sci.*, **38**, 1, 45–53, 1990.

Newnham, D. A. and Balard, J.: Visible absorption cross sections and integrated absorption intensities of molecular oxygen (O_2 and O_4), *J. Geophys, Res.*, **103(D22)**, 28801-28815, 1998.

Noxon, J. F.: Effect of Internal Gravity Waves Upon Night Airglow Temperatures, *Geophys. Res. Lett.*, **5**, 25–27, 1978.

Ogryzlo, E. A., Shen, Y. Q., and Wassel, P. T.: The yield of $O_2(b^1\Sigma_g^+)$ in oxygen atom recombination, *J. Photochem.*, **25**, 389, 1984.

Picone, J. M., Hedin, A. E., Drob, D. P., and Aikin, A. C.: NRLMSISE-00 empirical model of the atmosphere: Statistical comparisons and scientific issues, *J. Geophys, Res.*, **107**, 1468, doi:10.1029/2002JA009430, 2002.

Rodrigo, R., Lopez-Gonzalez, M. J., and Lopez-Moreno, J. J.: Variability of the neutral mesospheric and lower thermospheric composition in the diurnal cycle, *Planet. Space Sci.*, **39**, 803, 1991.

Shepherd, M. G., Cho, Y.-M., Shepherd, G. G., Ward, W., and Drummond, J. R.: Mesospheric temperature and atomic oxygen response during the January 2009 major stratospheric warming, *J. Geophys. Res.*, **115**, A07318, doi:10.1029/2009JA015172, 2010.

Slanger, T. G. and Black, G.: Interactions of $O_2(b^1\Sigma_g^+)$ with $O(^3P)$ and O_3. *J. Chem. Phys.*, **70**, 3434-3438, 1979.

Slanger, T. G., Bischel, W. K., and Dyer, M. J.: Photoexcitation of O_2 at 249.3 nm, *Chem. Phys. Lett.*, **108**, 472, 1984.

Smith, A. K., Marsh, D. R., Mlynczak, M. G., and Mast J. C.: Temporal variation of atomic oxygen in the upper mesosphere from SABER, *J. Geophys. Res.*, **115**, D18309, doi:10.1029/2009JD013434, 2010.

Smith, I. W. M.: The role of electronically excited states in recombination reactions, *Int. J. Chem. Phys.*, **16**, 423–443, 1984.

Strelnikov, B., Rapp, M., and Lübken, F.-J.: In-situ density measurements in the mesosphere/lower thermosphere region with the TOTAL and CONE instruments, in: An Introduction to Space Instrumentation, edited by: Oyama, K., Terra Publishers, doi:10.5047/isi.2012.001, 2013. http://www.terrapub.co.jp/onlineproceedings/ste/aisi/

536

537 Strelnikov, B., Staszak, T., Strelnikova, I., Lübken, F.-J., Grygalashvyly, M., Hedin, J.,
538 Khaplanov, M., Gumbel, J., Fasoulas, S., Löhle, S., Eberhart, M., Baumgarten, G., Höffner,
539 J., Wörl, R., Rapp, M., and Friedrich, M.: Simultaneous in situ measurements of small-scale
540 structures in neutral, plasma, and atomic oxygen densities during WADIS sounding rocket
541 project, *Atmos. Chem. Phys.*, submitted , 2018.

542

543 Takahashi, H., Sahai, Y., and Teixeira, N. R.: Airglow intensity and temperature response to
544 atmospheric wave propagation in the mesopause region, *Adv. Space Res.*, **10**, 77–81, 1990.

545

546 Takahashi, H., Sahai, Y., Batista, P. P., and Clemesha, B. R.: Atmospheric gravity wave
547 effect on the airglow O_2(0,1) and OH(9,4) band intensity and temperature variations observed
548 from a low latitude station, *Adv. Space Res.*, **12(10)**, 131–134, 1992.

549

550 Takahashi, H., Onohara, A., Shiokawa, K., Vargas, F., Gobbi, D.: Atmospheric wave induced
551 O_2 and OH airglow intensity variations: effect of vertical wavelength and damping, *Ann.*
552 *Geophys*, **29**, 631–637, 2011.

553

554 Tarasick, D. W. and Shepherd, G. G.: Effects of gravity waves on complex airglow
555 chemistries. 2. OH emission, *J. Geophys. Res.*, **97**, 3195-3208, 1992.

556

557 Troe, J.: Predictive Possibilities of Unimolecular Rate Theory, *J. Phys. Chem.*, **83 (1)**, 114-
558 126, doi: 10.1021/j100464a019, 1979.

559

560 Viereck, R. A. and Deehr, C. S.: On the interaction between gravity waves and the OH Meinel
561 (6-2) and O_2 Atmospheric (0-1) bands in the polar night airglow, *J. Geophys. Res.*, **94**, 5397–

562 5404, 1989.

563

564 Wildt, J., Bednarek, G., Fink, E. H., Wayne, R. P.: Laser excitation of the $A^3\Sigma_u^+$, $A'^3\Delta_u$ and
565 $c^1\Sigma_{u-}$ states of molecular oxygen, *Chem. Phys.*, **156(3)**, 497-508, doi: 10.1016/0301-
566 0104(91)89017-5, 1991.

567

568 Witt, G., Stegman, J., Murtagh, D. P., McDade, I. C., Greer, R. G. H., Dickinson, P. H. G.,
569 and Jenkins, D. B.: Collisional energy transfer and the excitation of $O_2(b^1\Sigma_g^+)$ in the
570 atmosphere, *J. Photochem.*, **25**, 365, 1984.

571

572 Wraight, P. C.: Association of atomic oxygen and airglow excitation mechanisms, *Planet.*
573 *Space Sci.*, **30(3)**, 251-259, 1982.

574

575 Yankovsky, V. A., Martysenko, K. V., Manuilova, R. O., and Feofilov, A. G.: Oxygen
576 dayglow emissions as proxies for atomic oxygen and ozone in the mesosphere and lower
577 thermosphere, *J. Mol. Spectrosc.*, **327**, 209–231, doi:10.1016/j.jms.2016.03.006, 2016.

578

579 Young, R. A. and Sharpless, R. L.: Chemiluminescence and reactions involving atomic
580 oxygen and nitrogen, *J. Chem. Phys.*, **39**, 1071, 1963.

581

582 Young, R. A. and Black, G.: Excited state formation and destruction in mixtures of atomic
583 oxygen and nitrogen, *J. Chem. Phys.*, **44**, 3741, 1966.

584

585 Zagidullin, M. V., Khvatov, N. A., Medvedkov, I. A., Tolstov, G. I., Mebel, A. M., Heaven,
586 M. C., and Azyazov, V. N.: $O_2(b^1\Sigma_g^+)$ Quenching by O_2, CO_2, H_2O, and N_2 at Temperatures
587 of 300–800 K, *J. Phys. Chem.*, **121 (39)**, 7343-7348, doi: 10.1021/acs.jpca.7b07885, 2017.

Zhang, S. P., Wiens, R. H., and Shepherd, G. G.: Gravity waves from O_2 nightglow during the AIDA '89 campaign II: numerical modeling of the emission rate/temperature ratio, η, *J. Atmos. Terr. Phys.*, **55**, 377–395, 1993.

Atmos. Chem. Phys. Discuss., https://doi.org/10.5194/acp-2018-696
Manuscript under review for journal Atmos. Chem. Phys.
Discussion started: 12 October 2018

Atmospheric Chemistry and Physics Discussions

Table 1. List of reactions with corresponding reaction rates (for three-body reactions [cm^6 $molecule^{-2}$ s^{-1}] and for two-body reactions [cm^3 $molecule^{-1}$ s^{-1}]), quenching coefficients, and spontaneous emission coefficients (s^{-1}) used in the paper.

	Reaction	Coefficient	Reference
R1	$O + O + M \xrightarrow{\varepsilon k_1} O_2(b^1\Sigma_g^+) + M$	$k_1 = 4.7 \cdot 10^{-33}(300/T)^2$ $\varepsilon - unknown$	Campbel and Gray (1973)
R2	$O_2(b^1\Sigma_g^+) + O_2 \xrightarrow{k_2^{O_2}} products$	$k_2^{O_2} = 7.4 \cdot 10^{-17} T^{0.5} e^{-\frac{1104.7}{T}}$	Zagidullin et al. (2017)
R3	$O_2(b^1\Sigma_g^+) + N_2 \xrightarrow{k_2^{N_2}} products$	$k_2^{N_2} = 8 \cdot 10^{-20} T^{1.5} e^{\frac{503}{T}}$	Zagidullin et al. (2017)
R4	$O_2(b^1\Sigma_g^+) + O \xrightarrow{k_2^O} products$	$k_2^O = 8 \cdot 10^{-14}$	Slanger and Black (1979)
R5	$O_2(b^1\Sigma_g^+) \xrightarrow{A_1} O_2 + hv(762nm)$	$A_1 = 0.0834$	Newnham and Ballard (1998)
R6	$O_2(b^1\Sigma_g^+) \xrightarrow{A_2} O_2 + hv(total)$	$A_2 = 0.088158$	Yankovsky et al. (2016)
R7	$O + O + M \xrightarrow{\alpha k_1} O_2^* + M$	$\alpha - unknown$	
R8	$O_2^* + O_2 \xrightarrow{\gamma k_3^{O_2}} O_2(b^1\Sigma_g^+) + O_2$	$\gamma - unknown$	
R9	$O_2^* + O_2, N_2, O \xrightarrow{k_3^{O_2}, k_3^{N_2}, k_3^O} prod.$	$k_3^{O_2}, k_3^{N_2}, k_3^O - unknown$	
R10	$O_2^* \xrightarrow{A_3} O_2 + hv$	$A_3 - unknown$	

Table 2. Efficiencies α of the different excited states of O_2.

$O_2(c^1\Sigma_u^-)$	$O_2(A'^3\Delta_u)$	$O_2(A^3\Sigma_u^+)$	$O_2(^5\Pi_g)$	Reference
0.03	0.12	0.04	0.66	Wraight (1982), Smith (1984)
0.04	0.18	0.06	0.5	Bates (1988)
0.03	0.18	0.06	0.52	López-González et al. (1992a, b, c)

Table 3. Fitting coefficients for combined mechanism (Eq. 9) at different efficiencies.

	Low $\tilde{\varepsilon}$ Wraight (1982)	High $\tilde{\varepsilon}$ Bates (1988)	Averaged $\tilde{\varepsilon}$ (this work)
$\tilde{\varepsilon}$	0.015	0.03	0.022
$D_1 = \tilde{k}_3^O / \tilde{k}_3^{O_2}$	0.211	0.397	0.231
$D_2 = \tilde{\alpha}\tilde{\gamma}$	0.087	0.073	0.08

Atmos. Chem. Phys. Discuss., https://doi.org/10.5194/acp-2018-696
Manuscript under review for journal Atmos. Chem. Phys.
Discussion started: 12 October 2018

Atmospheric Chemistry and Physics Discussions

623 **Figures.**

624 Figure 1. Measurements of a) temperature (CONE), b) number density of air (CONE), c)
625 atomic oxygen concentration (FIPEX), d) volume emission at 762 nm (photometer).

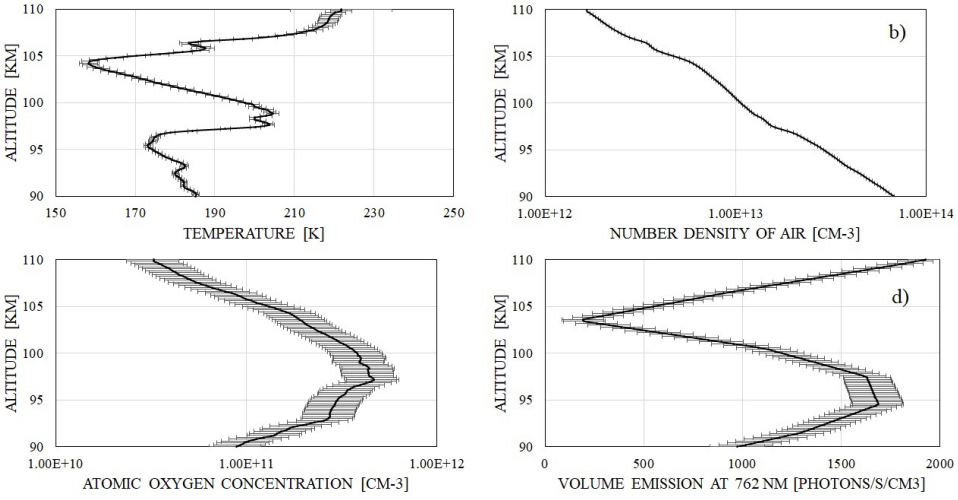

626
627
628
629
630
631
632
633
634
635
636
637
638
639
640

Atmos. Chem. Phys. Discuss., https://doi.org/10.5194/acp-2018-696
Manuscript under review for journal Atmos. Chem. Phys.
Discussion started: 12 October 2018

Atmospheric Chemistry and Physics Discussions

641 Figure 2. Fraction of recombination ε for the case of one-step mechanism.

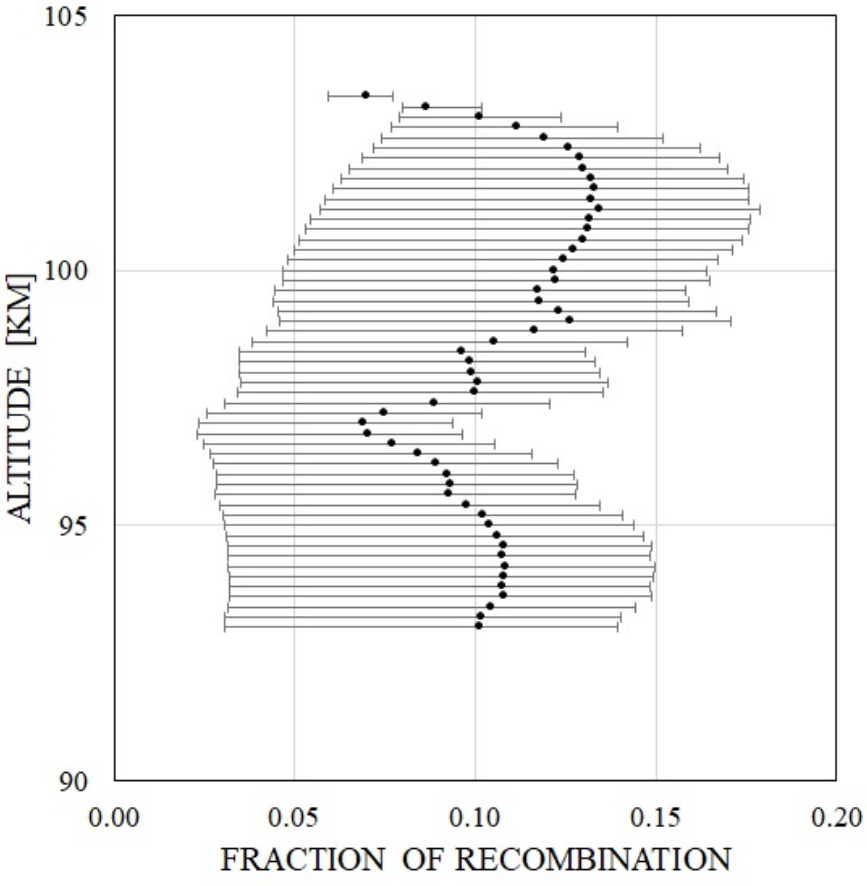

642

643

644

645

646

647

648

649

650

651

Atmos. Chem. Phys. Discuss., https://doi.org/10.5194/acp-2018-696
Manuscript under review for journal Atmos. Chem. Phys.
Discussion started: 12 October 2018

Atmospheric Chemistry and Physics Discussions

652 Figure 3. Correlation between fraction of recombination ε and T.

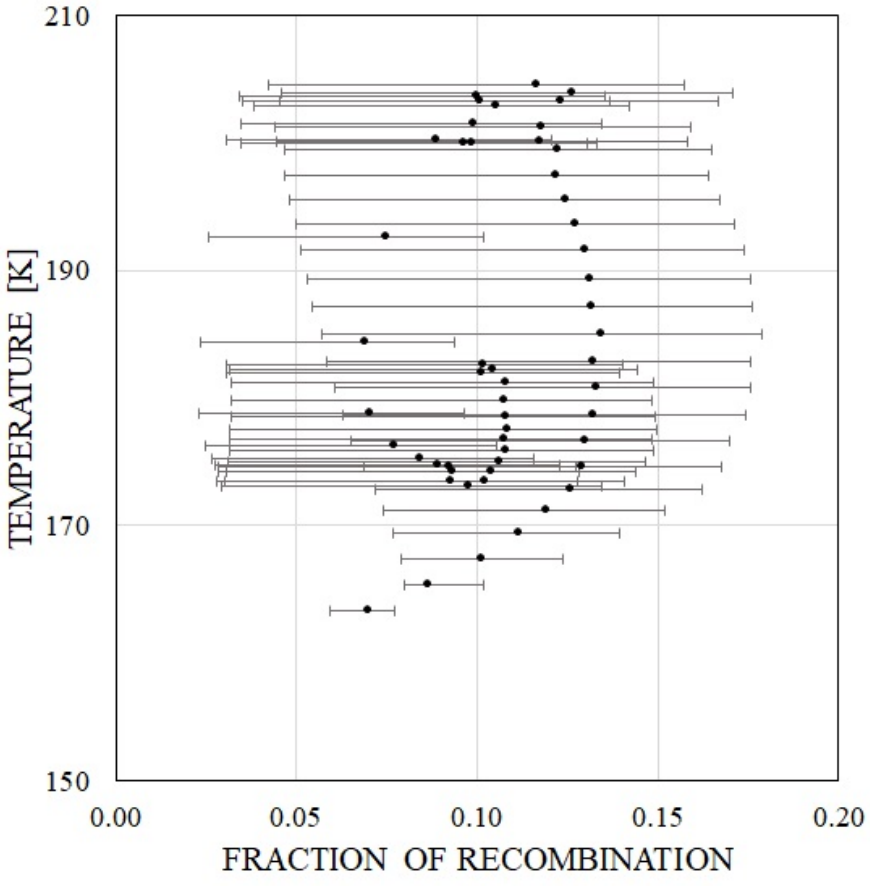

653

654

655

656

657

658

659

660

661

662

Atmos. Chem. Phys. Discuss., https://doi.org/10.5194/acp-2018-696
Manuscript under review for journal Atmos. Chem. Phys.
Discussion started: 12 October 2018

Atmospheric Chemistry and Physics Discussions

663 Figure 4. RHS of equation (8) and least-square fit of LHS of equation (8).

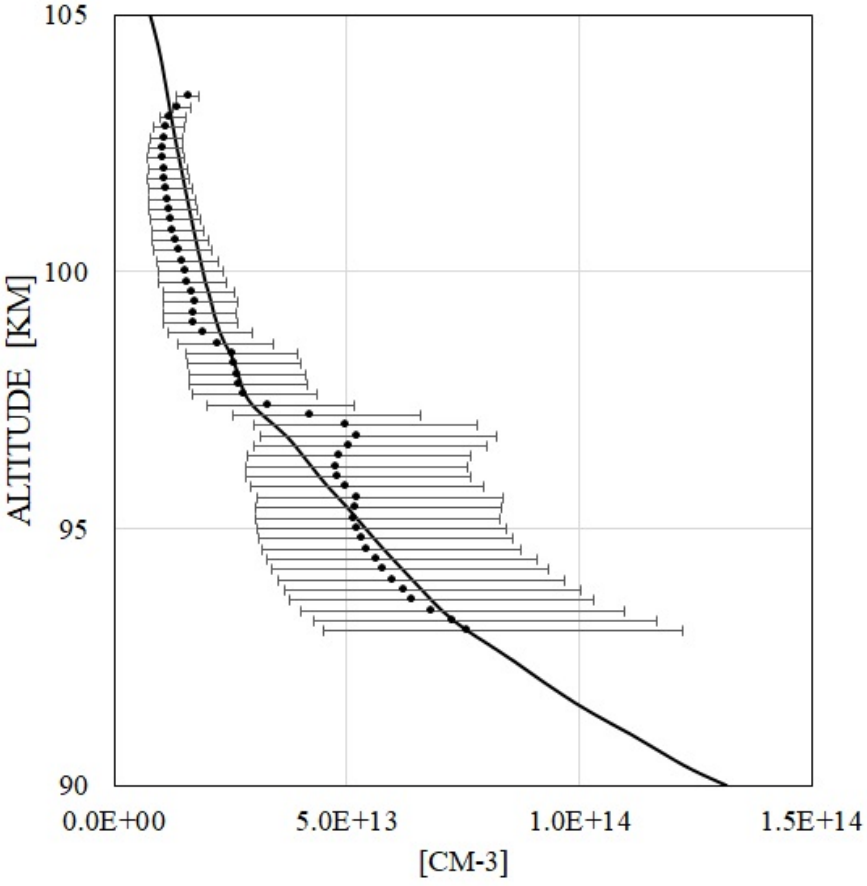

664

665

666

667

668

669

670

671

672

673

Atmos. Chem. Phys. Discuss., https://doi.org/10.5194/acp-2018-696
Manuscript under review for journal Atmos. Chem. Phys.
Discussion started: 12 October 2018

Atmospheric Chemistry and Physics Discussions

674 Figure 5. Atomic oxygen concentration: FIPEX (black line); model MSIS00 (red line);
675 derived from emission observation with McDade et al. (1986) coefficients (blue line);
676 calculated with newly derived fitting coefficients for the two-step mechanism (green line).

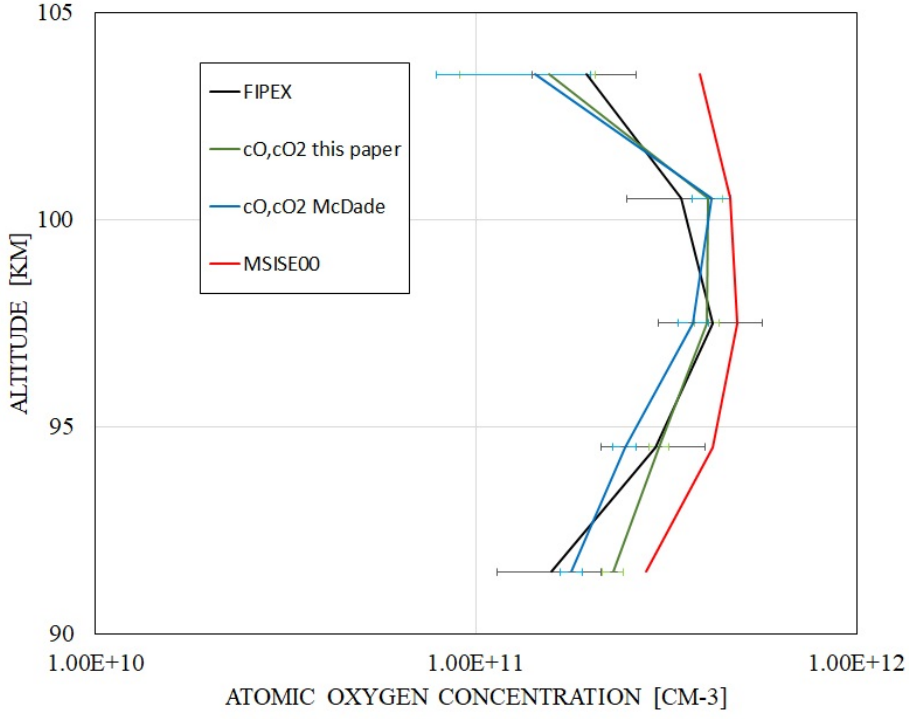

677
678
679
680
681
682
683
684
685
686
687

Atmos. Chem. Phys. Discuss., https://doi.org/10.5194/acp-2018-696
Manuscript under review for journal Atmos. Chem. Phys.
Discussion started: 12 October 2018

Atmospheric Chemistry and Physics Discussions

688 Figure 6. RHS and least-square fit of LHS of equation (9) for averaged case $\bar{\varepsilon}$=0.0225.

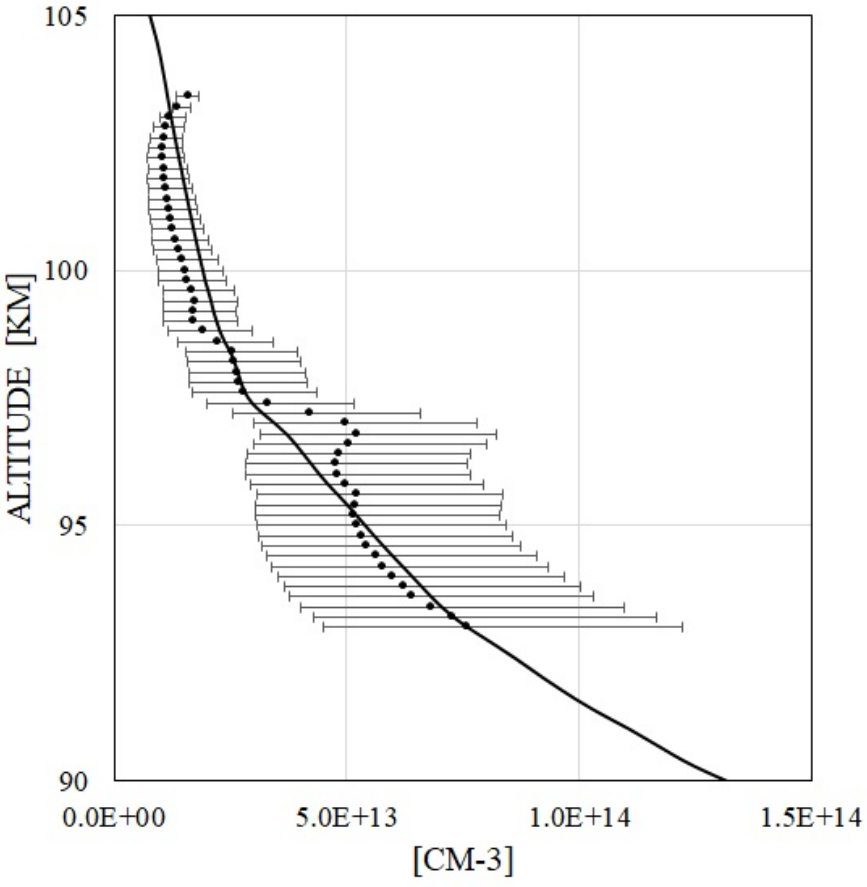

689

690

691

692

693

694

695

696

697

Atmos. Chem. Phys. Discuss., https://doi.org/10.5194/acp-2018-696
Manuscript under review for journal Atmos. Chem. Phys.
Discussion started: 12 October 2018

Atmospheric Chemistry and Physics Discussions

698 Figure 7. Volume emissions: photometer (red line); derived from atomic oxygen (black line)
699 with a) newly derived fitting coefficients for the two-step mechanism, b) with fitting
700 coefficients for combined mechanism, c) with McDade et al. (1986) coefficients, which
701 correspond to the MSIS-83 temperature, and with McDade et al. (1986) coefficients, which
702 correspond to the CIRA-72 temperatures.

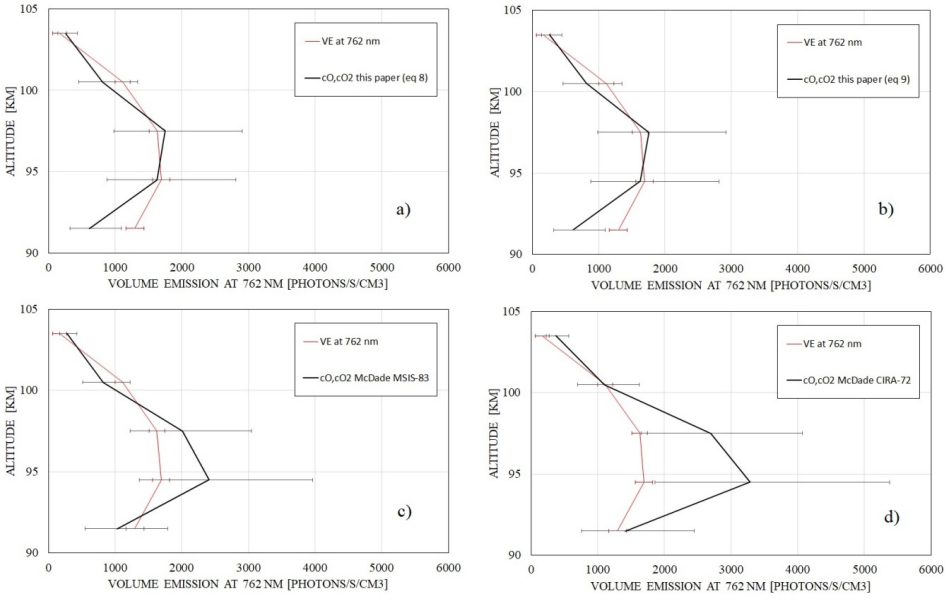

703